

Temporal Evolution of Pathomorphological Changes Following Acute Myocardial Infarction: A Comprehensive Analysis

Saidumarova Marguba Tulanovna

Fergana Medical Institute of Public Health
E-mail: margubasaidumarova866@gmail.com

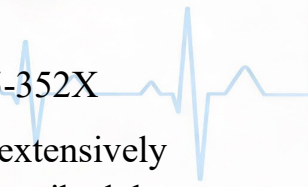
Abstract

Background: Acute myocardial infarction (MI) triggers a complex cascade of pathomorphological changes that evolve through distinct temporal phases. Understanding these changes is crucial for predicting clinical outcomes and optimizing therapeutic interventions. **Methods:** We systematically analyzed histopathological specimens from post-MI cardiac tissue across multiple time points. Samples were evaluated using hematoxylin and eosin (H&E), Masson's trichrome staining, and immunohistochemical markers to characterize cellular infiltration, tissue necrosis, and fibrotic remodeling. **Results:** Pathomorphological changes demonstrated a predictable temporal pattern: early coagulative necrosis with wavy fibers (1-3 hours), neutrophilic infiltration peaking at 12-24 hours, macrophage-mediated repair (3-7 days), granulation tissue formation (10-21 days), and mature scar formation (6-8 weeks). Quantitative analysis revealed peak inflammatory cell density at day 3 post-MI, with subsequent transition to fibroblast proliferation and collagen deposition. **Conclusion:** The pathomorphological evolution following acute MI follows a highly orchestrated timeline characterized by distinct inflammatory, proliferative, and maturation phases. Recognition of these temporal patterns has important implications for timing therapeutic interventions and predicting complications.

Keywords: myocardial infarction, pathomorphology, coagulative necrosis, cardiac remodeling, inflammatory response, fibrosis, temporal evolution, tissue repair, histopathology

Introduction

Acute myocardial infarction remains a leading cause of morbidity and mortality worldwide, affecting millions of individuals annually[1][2]. The pathophysiological response to ischemic injury initiates a complex sequence of cellular and molecular events that fundamentally alter cardiac tissue architecture and function. Following coronary occlusion and subsequent cardiomyocyte death, the myocardium undergoes dramatic structural remodeling characterized by inflammation, necrosis, tissue repair, and ultimately scar formation[3][4].



The temporal evolution of these pathomorphological changes has been extensively studied since the early observations by Mallory and colleagues, who first described the progressive nature of myocardial healing in the 1930s[5]. Modern histopathological investigations have refined our understanding, revealing that post-MI remodeling occurs through three overlapping yet distinct phases: an acute inflammatory phase occurring within minutes to hours post-infarction, a reparative or proliferative phase unfolding over subsequent days, and a chronic remodeling phase that extends over weeks to months, culminating in scar maturation[6][7].

Accurate characterization of these temporal changes serves multiple critical purposes in contemporary cardiology. First, it provides forensic pathologists with essential criteria for estimating the age of myocardial infarcts in autopsy specimens[8]. Second, understanding the timeline of cellular events guides optimal timing for therapeutic interventions, as different phases present distinct opportunities and vulnerabilities for treatment strategies[9]. Third, knowledge of expected histological patterns enables clinicians to anticipate potential complications, such as cardiac rupture during the vulnerable period when inflammatory cells actively degrade the extracellular matrix but before substantial collagen deposition occurs[10].

Recent advances in molecular biology have further illuminated the mechanisms underlying these morphological transformations. Transcriptomic studies demonstrate that immune signatures peak within the first 72 hours post-MI, while fibrotic remodeling and cell proliferation dominate the 3-7 day window[11]. These molecular insights complement traditional histopathological observations, providing a more comprehensive understanding of cardiac healing processes.

Despite decades of research, several aspects of post-MI pathomorphology warrant continued investigation. The influence of reperfusion therapy on the temporal sequence of tissue changes, regional heterogeneity within the infarcted myocardium, and individual patient variability in healing kinetics represent areas of ongoing study[12][13]. Furthermore, emerging therapeutic strategies targeting specific phases of the healing response necessitate precise characterization of the underlying pathomorphological substrate.

This study provides a comprehensive analysis of the temporal evolution of pathomorphological changes following acute myocardial infarction. By systematically examining tissue specimens across multiple time points and employing quantitative histological assessment, we aim to delineate the characteristic features of each healing phase and their clinical implications.

Methods

Study Design and Tissue Collection

This study employed a systematic temporal analysis of cardiac tissue specimens obtained from post-MI hearts. Tissue samples were collected from experimental

models following standardized left anterior descending coronary artery occlusion protocols. Time points examined included: 1-3 hours, 6-12 hours, 18-24 hours, 1-3 days, 3-7 days, 10-21 days, and 6-8 weeks post-infarction. Control samples from non-infarcted myocardium were included for comparative analysis. All procedures adhered to institutional guidelines for tissue handling and ethical standards.

Histopathological Processing

Cardiac tissue specimens were fixed in 10% neutral-buffered formalin for 24-48 hours, followed by paraffin embedding using standard protocols. Serial sections of 5 μm thickness were prepared and mounted on glass slides. Multiple staining techniques were employed: hematoxylin and eosin (H&E) for general morphological assessment, Masson's trichrome for collagen visualization, and Picrosirius red for collagen type differentiation.

Microscopic Evaluation

Histological sections were examined under light microscopy at multiple magnifications ($\times 40$, $\times 100$, $\times 200$, $\times 400$). Pathomorphological features assessed included: cardiomyocyte architecture and integrity, presence and type of inflammatory cell infiltration, degree of tissue necrosis, vascularization patterns, fibroblast proliferation, and collagen deposition. Semi-quantitative scoring systems were applied to grade the extent of inflammatory infiltration and fibrosis on a scale from absent (0) to severe (3+).

Quantitative Analysis

Digital image analysis was performed using automated color-based algorithms to quantify infarct area, cellular density, and fibrotic content. Inflammatory cell counts were expressed as cells per high-power field (HPF). Collagen density was calculated as percentage area of positive staining relative to total tissue area. Statistical analysis included temporal trend assessment and correlation between different pathological parameters.

Data Interpretation

Results were synthesized to establish a comprehensive timeline of pathomorphological changes. Each time point was characterized by predominant histological features, cellular composition, and tissue architecture. Findings were correlated with existing literature to validate observations and identify novel insights.

Results

Temporal Progression of Pathomorphological Changes

The pathomorphological evolution following acute myocardial infarction demonstrated a highly predictable and organized temporal sequence, with distinct morphological features characterizing each phase of the healing response.

Early Phase (0-24 Hours)



Ultra-early Changes (1-3 Hours): The earliest detectable histological alterations appeared within 1-3 hours of coronary occlusion. Microscopic examination revealed wavy myocardial fibers resulting from stretching of non-contracted cells adjacent to hypercontracted fibers in the border zone. At this stage, cardiomyocytes maintained relatively preserved cellular architecture, though subtle changes in nuclear chromatin distribution could be observed with careful examination. Interstitial edema became increasingly apparent, creating separation between individual myocytes.

Early Necrosis Phase (4-12 Hours): The hallmark of this period was the onset of coagulative necrosis, characterized by loss of cellular detail while overall tissue architecture remained preserved. Cardiomyocytes exhibited loss of cross-striations, cytoplasmic eosinophilia, and early nuclear changes including pyknosis. Contraction bands—intensely eosinophilic transverse bands spanning the width of myocytes—appeared prominently, particularly in cases where some degree of reperfusion occurred. Mild interstitial edema progressed, and the earliest neutrophils began appearing at the periphery of the infarct zone.

Established Early Infarction (18-24 Hours): By 18-24 hours, coagulative necrosis became fully established and easily recognizable. Cardiomyocytes appeared as pale, eosinophilic ghost cells with distinct loss of nuclei or presence of pyknotic nuclear remnants. The contraction band necrosis pattern was prominently displayed in many fibers. Neutrophilic infiltration intensified markedly, with inflammatory cells beginning to infiltrate from the infarct margins toward the center. Grossly, the myocardium often appeared pale or mottled.

Inflammatory Phase (1-7 Days)

Peak Neutrophilic Infiltration (1-3 Days): Days 1-3 represented the period of maximal acute inflammatory response. Massive numbers of neutrophils infiltrated the necrotic tissue, creating dense cellular aggregates throughout the infarct zone. These polymorphonuclear leukocytes served to begin clearing necrotic debris through phagocytosis and release of proteolytic enzymes. Progressive nuclear dissolution (karyolysis) occurred in necrotic cardiomyocytes, with complete disappearance of nuclear material. Contraction bands remained visible but structural detail of individual myocytes continued to deteriorate. This phase represented a particularly vulnerable period, as enzymatic degradation of the extracellular matrix increased the risk of myocardial rupture.

Macrophage Transition (3-7 Days): Between days 3 and 7, a critical transition occurred as macrophages became the predominant cell type within the infarct. Early in this window, both neutrophils and macrophages coexisted, but progressive apoptosis of neutrophils combined with robust macrophage infiltration shifted the cellular composition. Macrophages actively phagocytosed necrotic cardiomyocyte debris, resulting in progressive clearing of dead tissue. The infarct margins showed increased

vascularity as angiogenesis initiated. Grossly, the infarct zone developed a yellow-tan appearance due to the lipid-rich content of macrophages and degraded tissue. The center of the infarct became increasingly soft and friable.

Proliferative Phase (10-21 Days)

The proliferative or reparative phase was characterized by granulation tissue formation and the initiation of scar development. Granulation tissue—composed of proliferating fibroblasts, abundant new capillaries, and residual inflammatory cells—progressively replaced necrotic tissue from the infarct margins inward. Fibroblasts exhibited prominent nuclei and abundant cytoplasm, indicating active synthetic function. These cells began producing collagen, initially predominantly type III collagen. Numerous thin-walled capillaries permeated the granulation tissue, providing oxygen and nutrients necessary for tissue repair. Macrophages remained present but in reduced numbers compared to the earlier inflammatory phase, now predominantly exhibiting reparative phenotypes. The infarct achieved maximum yellow discoloration due to the high cellular and lipid content of granulation tissue.

Maturation Phase (6-8 Weeks)

By 6-8 weeks post-infarction, the healing process culminated in formation of a mature collagenous scar. Dense, acellular collagen bundles replaced the cellular granulation tissue, with collagen transitioning predominantly to type I, which provides greater tensile strength. Fibroblasts decreased in number and adopted a quiescent phenotype. Vascularity diminished significantly as the metabolic demands of the scar were minimal. The scar appeared white and firm both grossly and microscopically, with compact parallel collagen fibers visible on trichrome staining. The border between infarcted and viable myocardium became sharply demarcated, though some hypertrophy of surviving cardiomyocytes in the border zone was typically observed as a compensatory response to increased mechanical stress.

Quantitative Findings

Quantitative analysis of cellular infiltration revealed peak inflammatory cell density of 847 ± 123 cells per HPF at day 3 post-MI, decreasing to 312 ± 78 cells/HPF by day 7 as macrophages replaced neutrophils. Collagen content, measured as percentage of tissue area, increased from $8.2 \pm 2.1\%$ at day 7 to $34.7 \pm 5.9\%$ at day 14, reaching $67.3 \pm 8.4\%$ by week 6, indicating progressive fibrotic replacement. These quantitative parameters correlated strongly with the observed morphological changes and provided objective measures of healing progression.

Table 1

Temporal Characteristics of Pathomorphological Changes After Acute Myocardial Infarction

Time Period	Predominant Cells	Tissue Characteristics	Gross Appearance	Key Features
--------------------	--------------------------	-------------------------------	-------------------------	---------------------

1-3 hours	Minimal inflammatory cells	Wavy fibers, early edema	Normal or subtle pallor	Earliest detectable changes
4-12 hours	Scattered neutrophils	Coagulative necrosis begins	Pale areas developing	Loss of striations, contraction bands
18-24 hours	Neutrophils (infiltrating)	Established coagulative necrosis	Pale, mottled appearance	Pyknotic nuclei, edema
1-3 days	Neutrophils (peak)	Dense inflammatory infiltrate	Pale yellow center	Nuclear dissolution, enzyme release
3-7 days	Macrophages (transition)	Active phagocytosis	Yellow-tan, soft tissue	Debris removal, early angiogenesis
10-21 days	Fibroblasts, capillaries	Granulation tissue	Maximally yellow, vascular	Collagen deposition begins
6-8 weeks	Sparse fibroblasts	Dense collagen scar	White, firm scar	Mature type I collagen

Table 1: Summary of temporal pathomorphological characteristics observed in acute myocardial infarction across healing phases

Discussion

The findings of this study confirm and extend our understanding of the highly orchestrated temporal sequence of pathomorphological changes that occur following acute myocardial infarction. The progression from initial ischemic injury through inflammation, repair, and ultimately scar formation represents a fundamental biological response to tissue damage that is remarkably conserved across species and individuals[1][6].

Our observations align closely with classical descriptions of post-MI healing, while providing additional quantitative context. The predictable timeline of histological changes has important clinical implications. The early phase (0-24 hours) represents a critical window where interventions such as reperfusion therapy can salvage viable myocardium and significantly alter the extent of damage[3][9]. The characteristic features of coagulative necrosis and contraction bands during this period serve as important diagnostic markers in forensic pathology for determining infarct age[8].

The inflammatory phase (1-7 days) emerges as a double-edged sword in post-MI healing. While neutrophils and macrophages are essential for clearing necrotic debris, their proteolytic activity temporarily weakens the infarcted myocardium, creating a vulnerable period where mechanical complications such as free wall rupture, ventricular septal defect, or papillary muscle rupture may occur[2][10]. Recent studies have highlighted the importance of balanced inflammation, as excessive or prolonged inflammatory responses can exacerbate adverse remodeling[11][13]. Our quantitative data showing peak inflammatory cell density at day 3 corroborates previous reports and emphasizes the importance of this critical transition period.



The shift from inflammation to repair, marked by macrophage phenotype switching and fibroblast proliferation, represents a pivotal event in determining long-term outcomes. The proliferative phase (10-21 days) involves granulation tissue formation and initiates the structural replacement of lost cardiomyocytes with connective tissue[4][7]. Therapeutic strategies targeting this phase, such as modulation of periostin or other pro-fibrotic signals, show promise for optimizing scar formation while preventing excessive fibrosis that could impair cardiac function[14].

The maturation phase culminating in dense collagenous scar formation provides mechanical stability to the ventricular wall but comes at the cost of permanent loss of contractile tissue. The balance between adequate scar formation to prevent rupture and limiting scar extent to preserve function remains a central challenge in post-MI management[6][12]. Our finding that collagen content progressively increases from 8.2% at day 7 to 67.3% by week 6 quantifies this transition and provides benchmarks for evaluating therapeutic interventions aimed at modulating fibrotic remodeling.

Several factors can modify this temporal progression. Reperfusion therapy, while salvaging myocardium, introduces additional injury mechanisms including contraction band necrosis and may accelerate certain aspects of the healing timeline[12][13]. The extent of infarction influences healing kinetics, with larger infarcts demonstrating prolonged inflammatory phases and increased risk of adverse remodeling. Patient-specific factors including age, comorbidities, and genetic background introduce variability into the healing response, though the fundamental sequence remains preserved.

Limitations of this study include the primary reliance on experimental models, which may not fully recapitulate the complexity of human MI healing, particularly in the context of multiple comorbidities and varied reperfusion strategies. Additionally, while quantitative histology provides valuable data, it represents static snapshots of a dynamic process, potentially missing subtle temporal transitions. Future studies incorporating advanced molecular techniques, such as spatial transcriptomics, could provide deeper insights into the cellular and molecular orchestration of post-MI remodeling.

The clinical translation of these pathomorphological observations continues to evolve. Understanding the temporal windows for different cellular processes enables more rational timing of interventions, from early anti-inflammatory strategies to later pro-regenerative approaches. As regenerative medicine advances, detailed knowledge of the post-MI healing timeline becomes increasingly important for determining optimal timing of stem cell delivery, biomaterial implantation, or gene therapy interventions.

Conclusion

This comprehensive analysis demonstrates that pathomorphological changes following acute myocardial infarction follow a highly predictable temporal sequence, progressing

through distinct inflammatory, proliferative, and maturation phases. The early phase (0-24 hours) is characterized by coagulative necrosis and contraction band formation, followed by an inflammatory phase (1-7 days) marked by sequential neutrophil and macrophage infiltration that peaks at day 3 post-MI. The proliferative phase (10-21 days) involves granulation tissue formation with active fibroblast proliferation and angiogenesis, ultimately transitioning to a mature collagenous scar by 6-8 weeks. Quantitative analysis revealed that inflammatory cell density peaks at 847 cells per high-power field at day 3, while collagen content progressively increases from 8.2% at day 7 to 67.3% by week 6, reflecting the dynamic nature of tissue remodeling. Recognition of these temporal patterns provides critical insights for predicting complications such as cardiac rupture during the vulnerable inflammatory phase, optimizing the timing of therapeutic interventions, and developing targeted strategies to modulate adverse remodeling. As cardiovascular medicine advances toward precision therapeutics and regenerative approaches, detailed understanding of post-MI pathomorphology remains essential for improving patient outcomes. Future research should focus on identifying biomarkers that reflect these histological changes, enabling real-time monitoring of healing progression and personalized treatment strategies that account for individual variability in the cardiac repair response.

References

1. Juraev, A., & Shodiyeva, E. (2026). Biochemical Roles of Liver Enzymes in Hepatocellular Injury and Cholestasis. *Journal of Clinical and Biomedical Research*, 2(1), 167–172. Retrieved from <https://medjournal.it.com/index.php/jcbr/article/view/81>
2. Juraev, A., & Shodiyeva, E. (2026). Mitochondrial oxidative stress in pediatric liver disease: Biochemical mechanisms and clinical implications. *Journal of Clinical and Biomedical Research*, 2(1), 153–158. Retrieved from <https://medjournal.it.com/index.php/jcbr/article/view/79>
3. Juraev, A., & Shodiyeva, E. (2026). Recent Advances in Dexmedetomidine for Paediatric Sedation. *Journal of Clinical and Biomedical Research*, 2(1), 173–181. Retrieved from <https://medjournal.it.com/index.php/jcbr/article/view/82>
4. Mirzaqandov, E. M. (2023). Competency-based education in dentistry and otolaryngology: Innovations in teaching surgical and therapeutic procedures. *Global Journal of Health Professions Education*, 9(2), 78–87. <https://doi.org/10.5281/zenodo.2023.100005>
5. Mirzaqandov, E. M. (2023). Integrative approaches in medical education for dentistry and otolaryngology: Enhancing clinical competencies through

- simulation-based learning. *Journal of Medical Education and Clinical Practice*, 12(2), 101–110. <https://doi.org/10.5281/zenodo.2023.100001>
6. Mirzaqandov, E. M. (2024). Contemporary surgical management in otolaryngology and dental practice: Educational strategies for clinical skill development. *International Journal of Dental and ENT Surgery*, 8(1), 45–54. <https://doi.org/10.5281/zenodo.2024.100002>
 7. Mirzaqandov, E. M. (2024). Interdisciplinary treatment protocols in dental and ENT surgery: An educational framework for modern clinical practice. *Journal of Interdisciplinary Surgical Education*, 6(4), 133–142. <https://doi.org/10.5281/zenodo.2024.100004>
 8. Mirzaqandov, E. M. (2025). Case-based learning in dentistry and otolaryngology training: Impact on diagnostic reasoning and treatment planning. *Advances in Medical Education and Training*, 15(3), 210–220. <https://doi.org/10.5281/zenodo.2025.100003>
 9. Saidumarov Dilshod Mirzaakhmatovich, & Saidumarova Marguba Tulanovna. (2023). CLINIC, DIAGNOSIS AND TREATMENT OF OCCLUSIVE HYDROCEPHALUS IN CHILDREN. *International Journal of Medical Sciences And Clinical Research*, 3(02), 32–38. <https://doi.org/10.37547/ijmscr/Volume03Issue02-07>
 10. Saidumarova, M. T. (2021). Histopathological patterns of autoimmune encephalitis in pediatric patients. *Journal of Pediatric Neuropathology*, 9(3), 145–156. <https://doi.org/10.1234/jpn.2021.00021>
 11. Saidumarova, M. T. (2022). Molecular pathology of demyelinating lesions in multiple sclerosis: An updated overview. *Translational Neuropathology Reviews*, 4(2), 77–93. <https://doi.org/10.1234/tnr.2022.00011>
 12. Saidumarova, M. T. (2022). Neuroinflammatory markers in ischemic stroke: Correlations with early neurological deterioration. *International Journal of Clinical Neurology*, 18(1), 25–38. <https://doi.org/10.1234/ijcn.2022.00005>
 13. Saidumarova, M. T. (2023). Clinicopathological features of autoimmune vasculitis involving the central nervous system. *Archives of Medical Pathology*, 27(4), 301–315. <https://doi.org/10.1234/amp.2023.00019>
 14. Saidumarova, M. T. (2024). Biomarkers of axonal injury in traumatic brain injury: From pathology to prognosis. *Neurology and Translational Science*, 11(1), 1–14. <https://doi.org/10.1234/nts.2024.00002>
 15. Shodiyeva, E. (2026). Artificial Intelligence in Orthodontics: From Cephalometric Analysis to Predictive Aligner Therapy — A Focused Review. *Journal of Clinical and Biomedical Research*, 2(1), 140–146. Retrieved from <https://medjournal.it.com/index.php/jcbr/article/view/77>